

UNCLASSIFIED

Defense Technical Information Center
Compilation Part Notice

ADP011204

TITLE: The Influence of Non-Ideal Microstructures on the Analysis of Grain Boundary Impedances

DISTRIBUTION: Approved for public release, distribution unlimited

This paper is part of the following report:

TITLE: Internal Workshop on Interfacially Controlled Functional Materials: Electrical and Chemical Properties Held in Schloss Ringberg, Germany on March 8-13, 1998

To order the complete compilation report, use: ADA397655

The component part is provided here to allow users access to individually authored sections of proceedings, annals, symposia, etc. However, the component should be considered within the context of the overall compilation report and not as a stand-alone technical report.

The following component part numbers comprise the compilation report:
ADP011194 thru ADP011211

UNCLASSIFIED



ELSEVIER

Solid State Ionics 131 (2000) 117–127

**SOLID
STATE
IONICS**

www.elsevier.com/locate/ssi

The influence of non-ideal microstructures on the analysis of grain boundary impedances

J. Fleig*

Max-Planck-Institut für Festkörperforschung, Stuttgart, Germany

Received 1 November 1998; received in revised form 20 December 1998; accepted 10 January 1999

Abstract

The so-called brick layer model is frequently used to analyze impedance spectra of polycrystalline samples with highly resistive grain boundaries. However, the basic assumptions of the model (cubic grains, laterally homogeneous grain boundaries, identical properties of all grain boundaries) are usually violated in real ceramics. To investigate the impact of some deviations from the brick layer model, the potential distributions, and thus the impedance of polycrystals, have been calculated by the finite element method. The results show that bulk properties can distinctly influence the size and shape of the so-called 'grain boundary semicircle', particularly for laterally inhomogeneous grain boundaries and for properties varying from boundary to boundary. Depressions of the grain boundary semicircle solely due to a non-brick-layer microstructure are observed. The validity and limits of the brick layer model are discussed. © 2000 Elsevier Science B.V. All rights reserved.

Keywords: Grain boundaries; Microstructure; Impedance; Electrical properties; Brick layer model; Potential distribution

1. Introduction

Highly resistive grain boundaries are of great technological importance with regard to the overall electrical properties of polycrystalline materials and can play a desired functional role in semiconducting electroceramic devices such as varistors, thermistors and capacitors [1,2]. On the other hand, for many applications of solid electrolytes (e.g. fuel cells, oxygen pumps or electrochemical reactors) the overall conductivity of the electroceramic material should be as high as possible and highly resistive grain boundaries, such as those found in oxygen conduct-

ing membranes of zirconia [3–7], are distinctly unwelcome.

Impedance spectroscopy is an important tool to investigate the electrical properties of highly resistive grain boundaries since the grain boundaries frequently cause an additional semicircle in the complex impedance plane [3–7]. In order to analyze and interpret the spectra a brick layer model (Fig. 1a) is usually applied assuming cubic grains and laterally homogeneous as well as identical grain boundaries. However, these brick layer assumptions are more or less violated in real ceramics and a detailed investigation of the impact of such deviations on the overall impedance is still missing.

In this contribution an overview of impedance effects caused by some important deviations from the

*Tel.: +49-711-689-1770; fax: +49-711-689-1722.

E-mail address: fleig@chemix.mpi-stuttgart.mpg.de (J. Fleig)

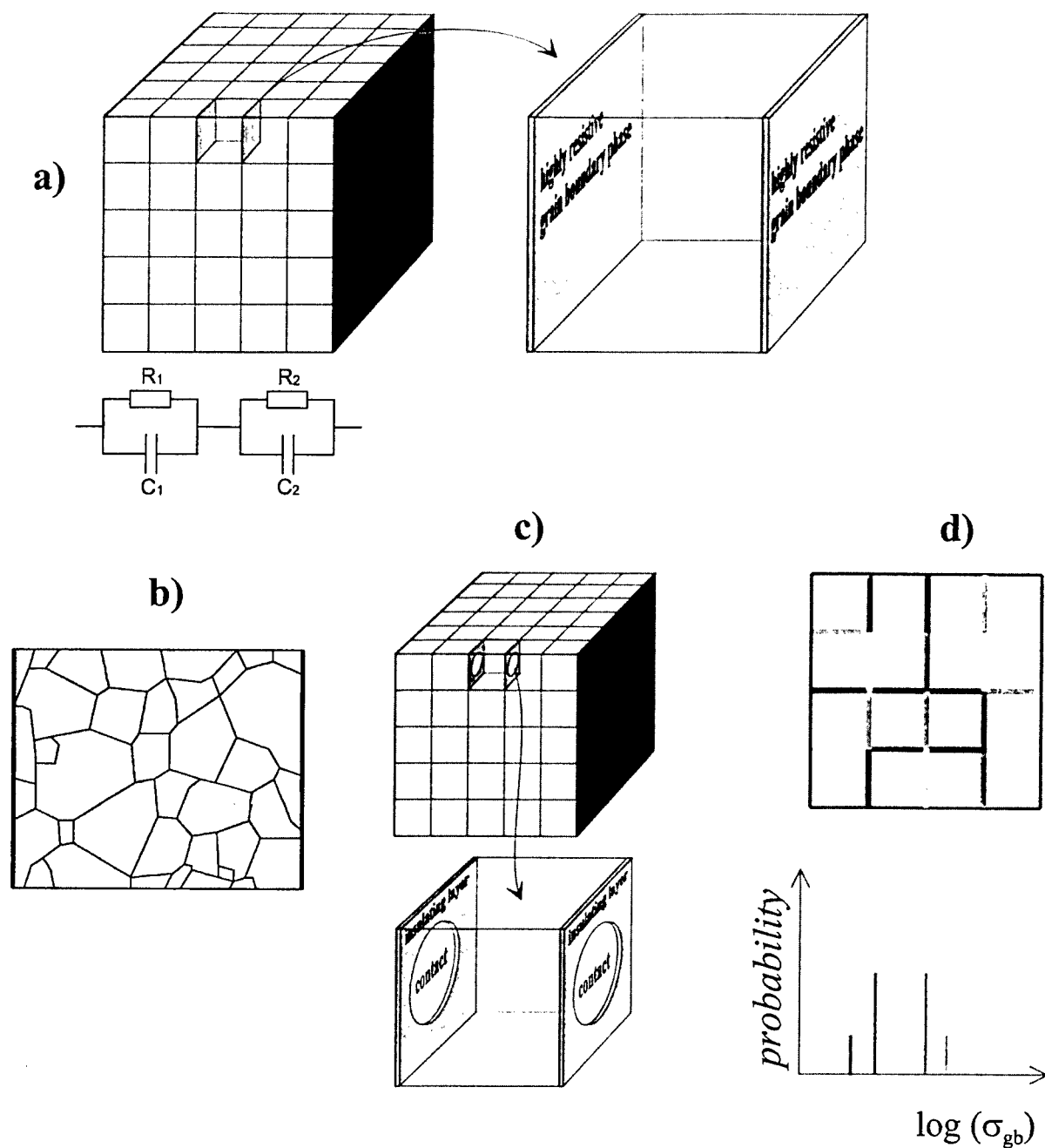


Fig. 1. Sketch of the brick layer model (a) and important deviations in real materials as considered in this contribution: (b) non-cubic grains (here in 2D); (c) laterally inhomogeneous grain boundaries (here in 3D); (d) grain boundary properties differing from grain to grain according to the probability distribution of the grain boundary conductivity (here in 2D). In the brick layer approach (a) highly resistive grain boundaries perpendicular to the electrodes can be neglected leading to the equivalent circuit shown in (a).

brick layer model is given, while a detailed analysis of some special aspects is presented elsewhere [8–10]. Particularly, we consider: (i) deviations from the cubic grain shape; (ii) the influence of imperfect contacts between the grains; and (iii) the impact of a distribution of different grain boundaries in the crystal (Fig. 1). Moreover, some conditions are discussed within which the brick layer model is a useful tool to estimate electrical properties of grain boundaries.

2. Model considerations

The potential distribution within a polycrystal is obtained by solving Laplace's equation for the electrical potential (φ). The impedance in a sample with bulk conductivity σ_{bulk} and permittivity ϵ_{bulk} can be calculated by integrating the complex current density, $j = -(\sigma + i\omega\epsilon)\text{grad}(\varphi)$, along an electrode. Grain boundaries are assumed to exhibit an effective thickness w_{gb} and an effective conductivity σ_{gb} . The microscopic reason for the blocking character of the grain boundary (e.g. core effects, space charge effects or a second phase) is not considered in this work.

In the case of the two-dimensional calculations of different grain boundary patterns (Section 3.1) identical grain boundary conductivity and thickness were assumed for all grain boundaries. In Section 3.2, in which the three-dimensional simulations of imperfect grain-to-grain contacts are discussed, the properties vary along a single grain boundary: the grain boundary conductivity is assumed to be zero for an insulating grain boundary phase (e.g. a solid phase or pores, Fig. 1c) and non-zero for the contacted region. In Section 3.3 (two-dimensional simulations) a variation in the conductivity from grain boundary to grain boundary was considered, using different probability distributions of σ_{gb} (cf. Fig. 1d).

The numerical solution was computed using the finite element software 'FLUX-EXPERT' from Simulog (1 Rue James Joule, 78280 Guyancourt Cedex, France). The grain boundaries may be taken into account via so-called 'interfacial elements' [9,11]. Further details on such calculations are given in Refs. [9,12].

3. Results and discussion

3.1. The influence of different grain boundary patterns

To examine the influence of the microstructure, FE-calculations in two dimensions were performed. A general principle may improve the experimentalists' prediction of the possible impact a given microstructure will have on the impedance: if possible, current lines make detours around hindrances, i.e. resistive grain boundaries. This leads to an interesting observation. Detours are 'easy' for high bulk conductivity, and excess grain boundaries are avoided. However, detours are 'difficult' for low bulk conductivity, and additional grain boundaries must be passed, leading to a greater grain boundary resistance than for the case of high σ_{bulk} [9]. Hence, the low-frequency semicircle of the impedance spectrum, which is usually exclusively interpreted in terms of grain boundary properties, can also be influenced by properties of the grain interior.

Such detour-effects can play an important role in real ceramics, particularly if broad grain size distributions exist or if the grain size distribution is spatially inhomogeneous. This is illustrated for a sample with inhomogeneous grain size distribution, as shown in Fig. 2 (consisting of some 7- μm large grains and agglomerations of smaller grains with 1- μm grain size). A simple calculation of an average grain size by counting the grains per area leads to a value of 1.94 μm . The low-frequency semicircle as obtained by finite element calculations is considerably smaller than predicted by the brick layer model for a grain size of 1.94 μm (see Fig. 2). As a consequence, the calculation of a meaningful average grain size requires a weighting in favour of large grains.

This can easily be understood from a plot of the magnitude of the d.c. current density (Fig. 3a): the current by-passes the regions of high grain boundary density and thus the inhomogeneous current distribution prefers large grains. However, this changes for relatively low bulk conductivity since detours become more difficult and a much more homogeneous current distribution results as shown in Fig. 3b. Hence the 'grain boundary resistance' as obtained from the low-frequency semicircle, depends

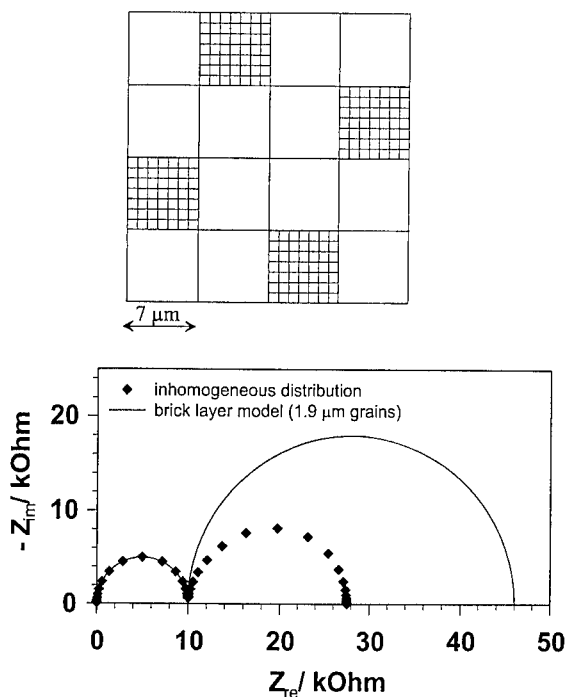


Fig. 2. Artificial microstructure representing the case of an inhomogeneous grain size distribution (agglomeration of smaller grains) and the resulting impedance spectrum as calculated by the finite element method. For comparison the spectrum calculated by assuming a brick layer model of 1.94 μm grain size is plotted as well. The grain boundary properties are: $\sigma_{\text{gb}} = 4 \times 10^{-8} \text{ } 1/\Omega$, grain boundary thickness = 2.8 nm, permittivity $\epsilon_{\text{gb}} = \epsilon_{\text{bulk}}$, bulk conductivity $\sigma_{\text{bulk}} = 10^{-4} \text{ } 1/\Omega$. (Please note, that in 2D the unit of a conductivity is $1/\Omega$.)

not only on the conductivity of the highly resistive grain boundaries but also on the bulk conductivity (Fig. 3c). As a consequence, the temperature-dependence of the low-frequency semicircle ('grain boundary semicircle') yields an apparent activation energy which can differ slightly from the true grain boundary activation energy. We give a numerical example for the case considered in Figs. 2 and 3: (i) if $E_{\text{act,bulk}} = 0.9 \text{ eV}$ and $E_{\text{act,gb}} = 1.8 \text{ eV}$ there is a 'medium' temperature regime with an apparent grain boundary activation energy of 1.7 eV. ('Medium' temperature regime means temperatures for which the sizes of the two semicircles are of the same order of magnitude.) The relative deviation from $E_{\text{act,gb}}$ can be shown to be approximately proportional to $(1 - E_{\text{act,bulk}}/E_{\text{act,gb}})$ and thus can be rather large for small $E_{\text{act,gb}}$.

Moreover, the low frequency semicircle is not ideal but asymmetrically distorted. A fit using a resistor in parallel with a constant phase element with impedance $Q^{-1}(i\omega)^{-n}$ ($Q, n = \text{fit parameters}$, $\omega = \text{angular frequency}$) yields a value of $n = 0.916$ for the left half of the low-frequency semicircle while the right half results in $n = 0.99$. It has to be emphasized that the depression is not due to a distribution of relaxation times (only one grain boundary relaxation time exists) but is instead a consequence of the frequency-dependence of the current lines: for low frequencies the current detours the excess grain boundaries, while for high frequencies the interfaces are nearly dielectrically short-circuited and a homogeneous current distribution results. This frequency-dependent switching of the current lines leads to modifications in the spectra shape and has no counterpart in quasi-one-dimensional systems as the simple brick layer model. The high-frequency semicircle, on the other hand, is not affected by the microstructural pattern and reveals the true bulk properties.

On the other hand, in many cases the brick layer model does allow reasonable estimates of the grain boundary properties. This is discussed in more detail in Ref. [9]. From the calculations therein (e.g. a pattern as shown in Fig. 1b) and other calculations for two-dimensional grain boundary patterns we expect that the brick layer model is a reasonable approximation for homogeneous and relatively narrow distributions of grain sizes and grain shapes. Serious problems are expected, for example, for a very broad grain size distribution with very large and very small grains or a spatially inhomogeneous grain size distribution as sketched in Fig. 3.

3.2. The influence of imperfect contacts

Grain boundaries are often laterally inhomogeneous (i.e. 'imperfect') in the sense that ideally conducting as well as totally insulating interface regions are present. To give two examples: (i) solid grain boundary phases frequently only partially wet the grains establishing a diminished grain-to-grain contact, and (ii) nanopores along grain boundaries can cause an imperfect contact between two grains. In such cases an insulating layer partly separates neighboring grains (Fig. 1c) and the d.c. current is

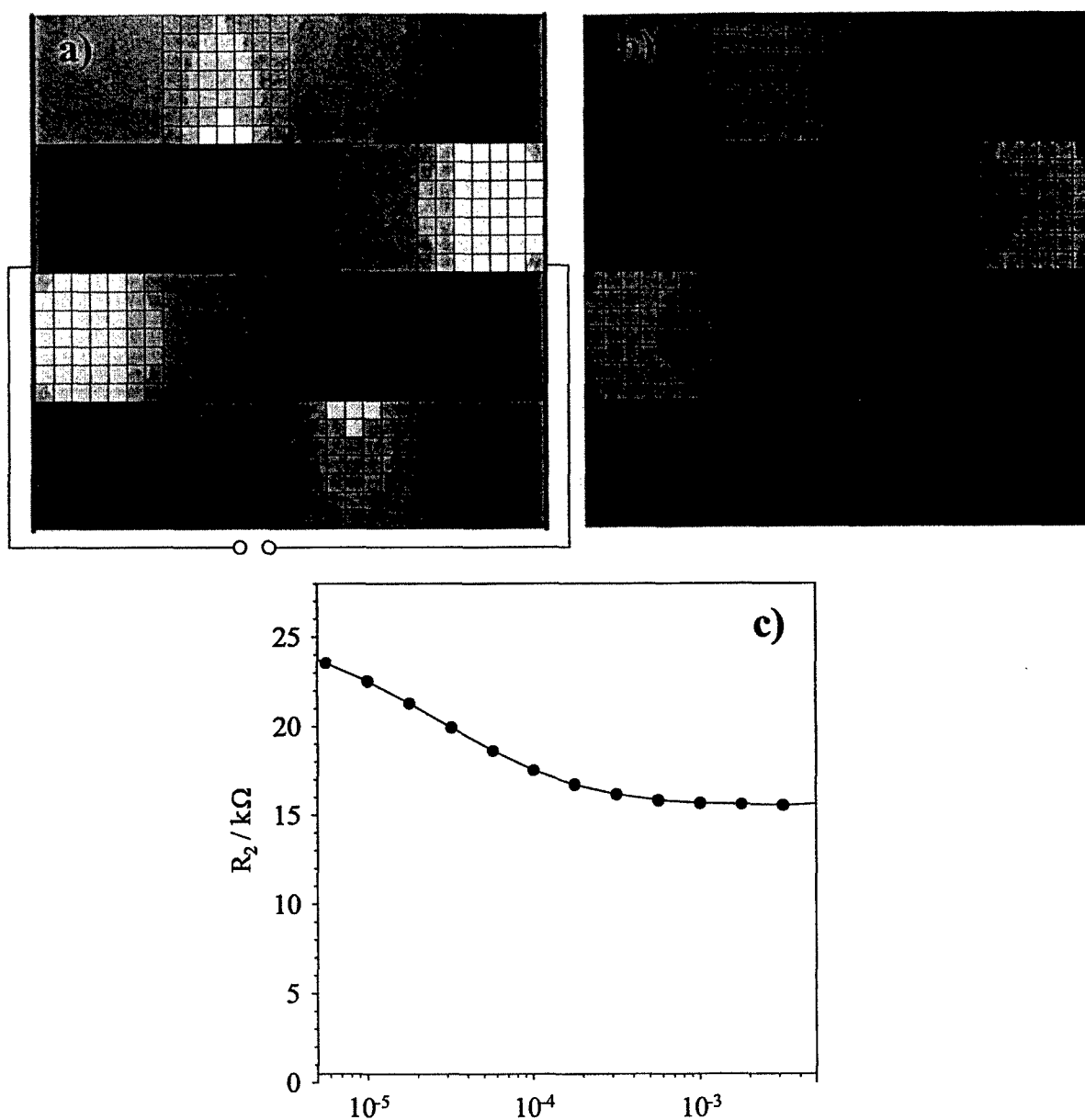


Fig. 3. Top: magnitude of the d.c. current density within the two-dimensional polycrystal of Fig. 2 for two different bulk conductivities: (a) $\sigma_{\text{bulk}} = 2 \times 10^{-4} \text{ } 1/\Omega$; (b) $\sigma_{\text{bulk}} = 10^{-5} \text{ } 1/\Omega$. For other parameters see Fig. 2. Dark indicates high current density and light low current density. Bottom: resistance from the low-frequency semicircle R_2 as a function of bulk conductivity.

constricted close to the conducting grain-to-grain contacts. Consequently the d.c. bulk resistance is higher than the ideal bulk resistance. Such imperfect contacts give rise to a low-frequency semicircle in the complex impedance plane (Fig. 4) which can be

interpreted in terms of a transition of the bulk resistance from the d.c. value to the a.c. (ideal) value due to the dielectric 'opening' of the insulating grain boundary phase capacitor [8]. Hence it is not the sequence of two serial regions of different conduc-

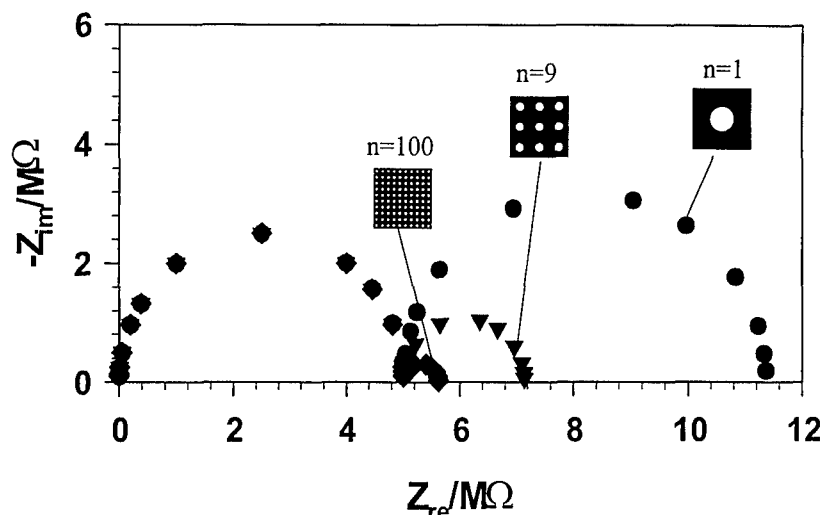


Fig. 4. Impedance spectra for a three-dimensional polycrystal (bulk conductivity $\sigma_{\text{bulk}} = 10^{-7} \text{ } 1/\Omega \text{ cm}$) with an electrode area of 1 cm^2 and a thickness of 5 mm . All grain boundaries are identical but laterally inhomogeneous, consisting of an insulating phase (thickness = 2 nm , permittivity = ϵ_{bulk}) and different amounts (n) of circular perfectly conducting spots (cf. Fig. 1c). The insets sketch cross-sections of the grain boundaries between two grains (cf. Fig. 1c) with contacted (white) and insulating (black) regions. In all three cases the fraction of contacted area per grain boundary is kept constant at 12.6% . The dc resistance ($11.4 \text{ m}\Omega$) is a pure bulk resistance and is larger than the ideal bulk resistance ($5 \text{ M}\Omega$) because of the current constriction close to the contacted spots.

tivities but the frequency-dependent shift of the current lines that leads to the low-frequency semicircle. Fig. 4 shows the resulting impedance spectra for different grain boundary contact geometries, all of them exhibiting the same area fraction of insulating grain boundary phase ($-\alpha_{\text{contact}}$) but different numbers of contact spots carrying the d.c. current. The so-called 'grain boundary resistance' R_2 (diameter of the low-frequency arc) strongly depends on the number of contacts while the high-frequency semicircle is not influenced by grain boundary properties and still reveals the 'ideal' bulk values as expected for a single crystal. It has to be emphasized that the additional resistance is not due to the contact 'bridge' which connects two grains (cf. Fig. 1c) but is caused by the current constriction in the grain bulk close to the conducting grain-to-grain contacts.

A quantitative estimate of the magnitude of the 'grain boundary resistance' R_2 is possible according to Ref. [8]

$$R_2 \approx \frac{1}{\sigma_{\text{bulk}}} \frac{1}{\sqrt{4\alpha_{\text{contact}}n}} \frac{L_{\text{sample}}}{A_{\text{sample}}} \quad (1)$$

In Eq. (1) n is the number of grain-to-grain

contacts per grain boundary and α_{contact} the fraction of established contact area (contacted area/complete area), σ_{bulk} denotes the bulk conductivity and L_{sample} , A_{sample} are the sample thickness and area, respectively. Thus R_2 is determined by two independent parameters ($\alpha_{\text{contact}}, n$), and an evaluation of the contacted area (or of the fraction of 'blocked' current) solely from the impedance spectrum is not possible. The 'grain boundary capacitance', on the other hand, allows an estimate of the thickness of the insulating grain boundary phase [8].

To help estimate to what extent current constriction might cause grain boundary impedances in real electroceramic materials, a plot is given (Fig. 5) which relates R_2/R_1 (i.e. the ratio of the semicircle diameters) to the fraction of contacted area (α_{contact}) for varying contact numbers per grain boundary. From Fig. 5 and also from the estimate according to Eq. (1), it can be seen that pronounced low-frequency semicircles require rather small contact areas, particularly if many contact spots are involved. In many cases we expect the grain boundary resistance due to current constriction to be of the order of magnitude of the ideal bulk resistance or even

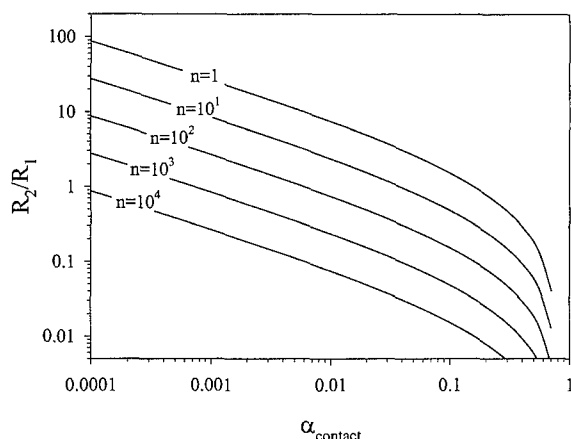


Fig. 5. Ratio of R_2/R_1 ('grain boundary resistance'/ideal bulk resistance) depending on the fraction of contacted area α_{contact} , for different numbers of contacts per grain boundary n . The plots are calculated using a more generally valid estimate than Eq. (1) as given in Ref. [8].

smaller. However, in porous material (e.g. freshly pressed samples) or if there are only very few gaps (pin-holes) in a highly resistive grain boundary phase current constriction effects can be considerably larger.

Indications that current constriction effects are relevant can be obtained from the temperature, partial pressure, bias and grain size dependence of R_2 . If current constriction plays a role, the temperature and partial pressure dependence of R_2 should be close to that of the bulk as already predicted by intuitive models [3,5–7,13]. A bias-dependent 'grain boundary resistance', on the other hand, suggests other mechanisms than current constriction. The grain size dependence of the grain boundary resistance, finally, is expected to deviate from the inverse linear relationship suggested by the brick layer model. Further information is given in Refs. [8,12].

However, the situation becomes more complicated if partially blocking and totally blocking interface regions exist simultaneously. For example, an insulating grain boundary phase partially wets the grains while at the established grain-to-grain contacts an additional transfer resistivity exists. Current constriction effects and 'true' grain boundary contributions due to the transfer process superimpose and lead to a rather complex situation.

To get a first insight into this topic we consider the following grain boundary case. A solid grain boundary phase (thickness 2 nm) partially wets the grains, leaving a circular grain-to-grain contact with a diameter of 54% of the grain boundary length (2 μm) (as sketched in Fig. 1c). At the established contact we assume a transfer hindrance which can be described by a 2-nm thick 'layer' of conductivity σ_{gb} and permittivity ϵ_{bulk} . As shown in Fig. 6, again one low-frequency semicircle arises in the complex impedance plane. However, this low-frequency semicircle includes both bulk contributions (due to current constriction) and 'true' grain boundary contributions owing to the partial blocking at the established contact. Hence a 'mixed' activation energy results and even a change of the activation energy with temperature from the bulk value to a higher or lower value (non-Arrhenius-behaviour) is possible. Nevertheless, the contribution of current constriction within the grains can be estimated by Eq. (1).

Such ambiguous situations arise if the capacitance of the insulating grain boundary phase is larger than the capacitance related to the transfer process at the established contact. Since relevant current constriction effects require relatively small contacted areas (see Fig. 5) we expect that this condition for the two

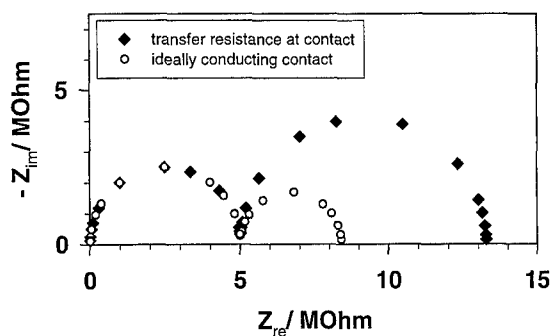


Fig. 6. Impedance spectra for a three-dimensional crystal (bulk conductivity $\sigma_{\text{bulk}} = 10^{-7} \text{ 1}/\Omega \text{ cm}$) with and without an additional transfer resistance at the established grain-to-grain contact. All grain boundaries are identical and exhibit one contact spot with contact area $\alpha_{\text{contact}} = 0.23$. Parameters: electrode area, 1 cm^2 ; sample thickness, 5 mm; thickness of the insulating phase, 2 nm; permittivity of the insulating phase, ϵ_{bulk} ; partial blocking at the established contact according to a 2-nm thick 'layer' of conductivity, σ_{gb} ; and permittivity, ϵ_{bulk} .

capacitances is often fulfilled at real grain boundaries. However, if the opposite situation is valid (capacitance of the insulating layer smaller than the transfer capacitance) a third semicircle appears, and an approximate separation of current constriction and true grain boundary resistance is possible, as shown for a similar problem (fuel cell cathode with the current being constricted close to the three phase boundary region) in Ref. [14].

3.3. The influence of the distribution of different grain boundaries in space

Even if each individual grain boundary is laterally homogeneous, the structural and chemical qualities, and thus the electrical properties, may vary from boundary to boundary leading to a certain distribution of grain boundary conductivities as sketched in Fig. 1d. One example where such a distribution is expected is for the case when the grain boundary resistance is caused by a space charge depletion layer. Due to an exponential relation, relatively small variations of the space charge potential result in strong variations of the effective grain boundary resistivity.

We probed the influence of distributions of different grain boundaries in two dimensions for some probability distributions of the grain boundary conductivity σ_{gb} (Figs. 7–9). Following the given distribution the grain boundary conductivities were randomly distributed in the square microstructural pattern (cf. Fig. 1d, the calculations are performed for a sample consisting of 10×10 grains).

Fig. 7 shows the spectrum for a discrete Gaussian distribution of $\log(\sigma_{gb})$ calculated by the finite element method and a spectrum according to the brick layer model using the 'mean' grain boundary conductivity ($10^{-7} \text{ 1}/\Omega$). Such a distribution of $\log(\sigma_{gb})$ corresponds to a Gaussian distribution of the space charge potential. Even though the extreme conductivity values of the distribution differ by a factor of 100 the brick layer model allows a rather satisfying estimate of the 'mean' grain boundary properties. However, again an inhomogeneous current distribution results which depends weakly on the bulk conductivity. Therefore, bulk properties slightly influence the 'grain boundary semicircle' (cf. Fig. 3), and a minor difference between the activation energy

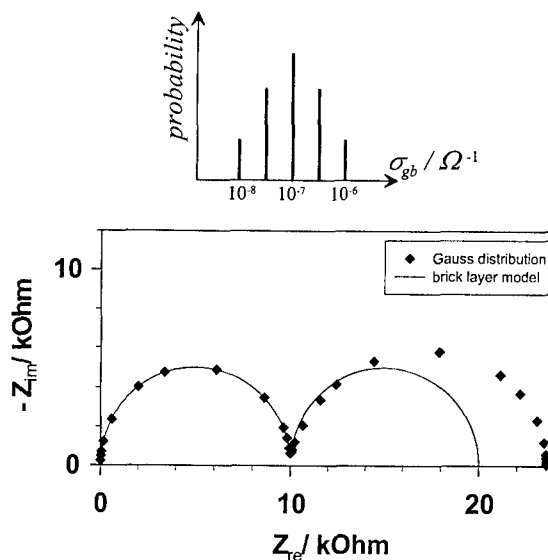


Fig. 7. Calculated impedance spectrum of a polycrystal (10×10 grains) for a discrete Gaussian distribution of the grain boundary conductivities (cf. Fig. 1d). The Gaussian distribution is on a logarithmic scale. The corresponding brick layer model assumes a conductivity according to the 'mean' value of the distribution ($10^{-7} \text{ 1}/\Omega$). Parameters: two-dimensional bulk conductivity, $10^{-4} \text{ 1}/\Omega$; grain size, $2 \mu\text{m}$; grain boundary thickness, 2 nm .

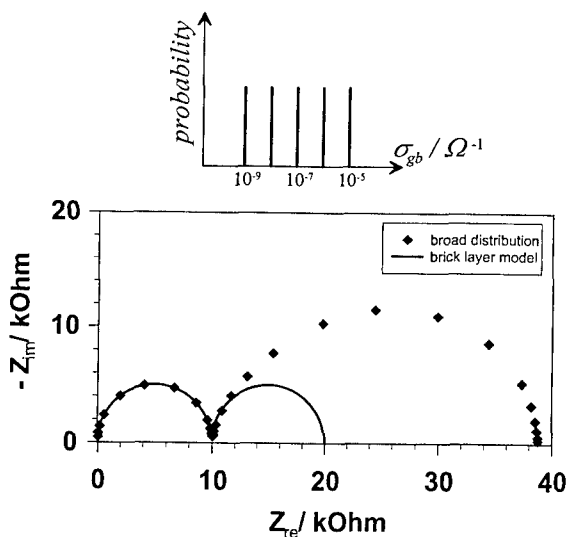


Fig. 8. Calculated impedance spectrum of a polycrystal (10×10 grains) for a very broad distribution of the grain boundary conductivity (cf. Fig. 1d). The corresponding brick layer model assumes a conductivity according to the center of the distribution ($10^{-7} \text{ 1}/\Omega$). Other parameters as in Fig. 7.

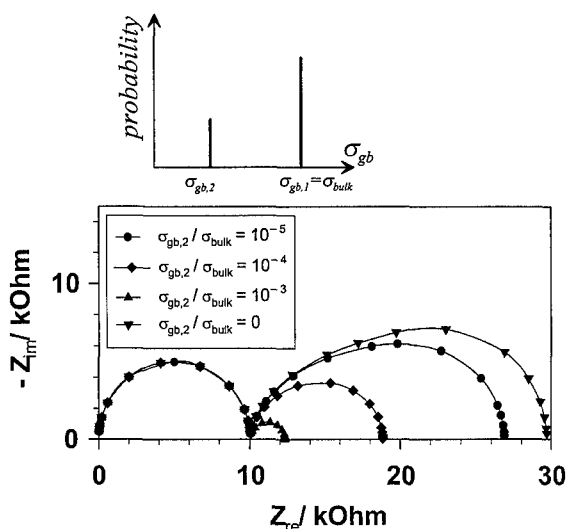


Fig. 9. Calculated impedance spectra of a polycrystal (10×10 grains) for different bimodal distributions of the grain boundary conductivity (cf. Fig. 1d). While 70% of the grain boundaries exhibit bulk conductivity $\sigma_{bulk} = \sigma_{gb,1} = 10^{-4} \text{ } 1/\Omega$, $\sigma_{gb,2}$ varies between $10^{-7} \text{ } 1/\Omega$ and zero. Other parameters as in Fig. 7.

of the low-frequency semicircle and the true activation energy of the grain boundary resistivity can occur. Moreover, the low-frequency semicircle exhibits a weak asymmetric depression (Fig. 7).

The situation becomes more difficult for a very broad conductivity distribution of constant probability (Fig. 8). A strongly deformed 'grain boundary semicircle' results and a brick layer model using the conductivity of the center of the distribution ($10^{-7} \text{ } 1/\Omega$) underestimates the 'grain boundary resistance' considerably. On the other hand, a serial connection of grain boundaries according to the given probability distribution yields a much larger value of R_2 than the two-dimensional distribution (222 k Ω). This again demonstrates the influence of detours around high-resistive grain boundaries to lower the resistance but also the problems to deduce a meaningful parameter from the 'grain boundary resistance'. Furthermore, the 'grain boundary resistance' is distinctly influenced by the bulk conductivity. As in the case of different grain boundary patterns (see Section 3.1), detour effects around very blocking grain boundaries contribute to the low-frequency 'semicircle'. Consequently the apparent activation energy no

longer reflects the activation energy of the grain boundary conductivity even if all σ_{gb} of the distribution have identical activation energies.

Let us finally discuss the extreme case in which 70% of the grain boundaries are ideal and exhibit bulk conductivity while 30% are highly resistive (bimodal distribution). Fig. 9 demonstrates, how the 'grain boundary arc' depends on the conductivity of the highly resistive interfaces ($\sigma_{gb,2}$). For moderate grain boundary conductivity the arc is semicircle-like and depends mainly on $\sigma_{gb,2}$ but only slightly on the bulk conductivity. For highly blocking grain boundaries, on the other hand, the low-frequency 'semicircle' becomes distinctly distorted and its size depends only weakly on $\sigma_{gb,2}$ but mainly on the bulk conductivity. In the extreme case of 30% totally insulating grain boundaries the low-frequency arc reaches a maximum and the so-called 'grain boundary resistance' turns out to be a part of the d.c. bulk resistance caused by detours around the very blocking grain boundaries. Hence the mechanism determining the resistance of the low-frequency arc changes with decreasing grain boundary conductivity and the apparent activation energy varies from the activation energy of $\sigma_{gb,2}$ to the bulk value for decreasing $\sigma_{gb,2}/\sigma_{bulk}$ ratio. This is demonstrated in Fig. 10 for bulk and grain boundary activation energies of 0.6 and 1.2 eV, respectively.

These examples demonstrate that, on one hand, a brick layer analysis can yield meaningful values as long as relatively narrow Gauss distributions of grain boundary properties are considered, while it can completely fail in other cases. A more detailed investigation in three dimensions is in progress [10] and will reveal more quantitatively the conditions under which a brick layer analysis is useful.

Finally we can conclude from Sections 3.1 to 3.3 that two- or three-dimensional current lines can depend on bulk conductivity and a.c. frequency. This leads to new features which do not exist in related one-dimensional problems as for example to bulk-dependent 'grain boundary semicircles' and to distorted or additional arcs only due to a change of the current lines with increasing frequency. As a consequence, the resistance of the low-frequency semicircle (R_2) does frequently not represent the exact resistance of the grain boundaries themselves. On the other hand, the term 'grain boundary resistance' is

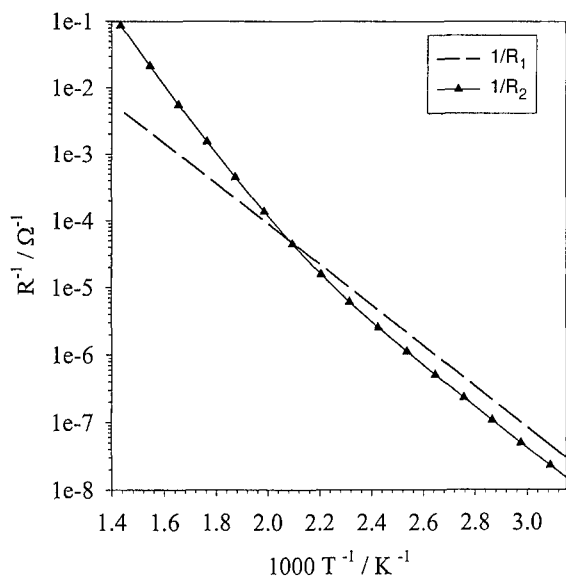


Fig. 10. Bulk (R_1) and 'grain boundary resistance' (R_2) for the bimodal distribution of grain boundary properties as shown in Fig. 9. The bulk conductivity σ_{bulk} has an activation energy of 0.6 eV while $\sigma_{\text{gb},2}$ is activated with 1.2 eV. Notice that $R_2^{-1}(T)$ reflects the activation energy of $\sigma_{\text{gb},2}$ at high temperatures, but $R_2^{-1}(T)$ approaches bulk activation at low temperatures.

still meaningful in the sense that R_2 is caused by the grain boundaries and does not exist in a corresponding single crystal.

However, in all cases the high-frequency semicircle reveals the ideal bulk values as expected for a single crystal, since for the entire high-frequency arc the grain boundaries are dielectrically conducting and hence negligible. This is even true if the d.c. resistance is a pure bulk resistance, i.e. if the low-frequency semicircle is caused by detours around blocking grain boundaries.

4. Conclusions

- Deviations from the cubic grain size are acceptable for a brick layer analysis as long as the grain size distribution is relatively narrow and spatially homogeneously, and as long as no pronounced anisotropy in the grain shape distribution exists. However, agglomerates of small grains or very

broad distributions can lead to considerable errors.

- If imperfect contacts (lateral inhomogeneities) between grains occur, current constriction in the grain becomes important. This leads to an apparent grain boundary semicircle, the resistance of which is purely bulk-dependent. An estimate of the additional resistance can be given according to Eq. (1), however, a quantitative determination of the fraction of blocked grain boundary area solely from the impedance spectrum is not possible. A simple brick layer analysis fails in such cases.
- The brick layer model can be used to estimate mean grain boundary properties if a relatively narrow (Gaussian) distribution of grain boundary conductivities is given. However, very broad or bimodal distributions lead to large deviations and a meaningful analysis using the brick layer model fails. In such cases the low-frequency arc can be distinctly influenced by bulk properties and considerably distorted. This can lead to apparent activation energies which differ from the true grain boundary activation energy.
- Grain boundary arcs deviating from ideal semicircles do not only occur for distributions of relaxation times, but also for microstructures which differ from the brick layer model even if only a single grain boundary relaxation time is involved.
- In all cases considered the high-frequency semicircle still reveals the ideal bulk resistance and capacitance as expected for a single crystal.

References

- [1] F. Greuter, G. Blatter, *Semiconduct. Sci. Tech.* 5 (1990) 111.
- [2] G. Pike, *Mater. Sci. Tech.* 11 (1994) 731.
- [3] J.E. Bauerle, *J. Phys. Chem. Solids* 30 (1969) 2657–2670.
- [4] T. van Dijk, A.J. Burggraaf, *Phys. Stat. Sol. (a)* 63 (1981) 229–240.
- [5] M.J. Verkerk, B.J. Middelhuys, A.J. Burggraaf, *Solid State Ionics* 6 (1982) 159.
- [6] S.P.S. Badwal, *Solid State Ionics* 76 (1995) 67.
- [7] M. Kleitz, H. Bernard, E. Fernandez, E. Schouler, *Advances in ceramics*, in: A.H. Heuer, L.W. Hobbs (Eds.), *Science and Technology of Zirconia*, Vol. 3, The American Ceramic Society, Washington, DC, 1981, p. 310.

- [8] J. Fleig, J. Maier, *J. Am Ceram. Soc.* 82 (1999) 3485.
- [9] J. Fleig, J. Maier, *J. Electrochem. Soc.* 145 (1998) 2081.
- [10] J. Fleig, J. Maier, (in preparation).
- [11] Les element interfaciaux dans FLUX-EXPERT Version 2.0, Simulog, 60 rue Lavoisier, 38330 Montbonnot, France, 1996.
- [12] J. Fleig, J. Maier, *J. Electroceramics* 1 (1997) 73.
- [13] P.G. Bruce, A.R. West, *J. Electrochem. Soc.* 130 (1983) 662.
- [14] J. Fleig, J. Maier, *J. Electrochem. Soc.* 144 (1997) L302.